Santa Clara University
Scholar Commons

Electrical Engineering
School of Engineering

6-1-1990

Properties and Device Applications of Hydrogenated Amorphous Silicon Carbide Films

M. Mahmudur Rahman

Cary Y. Yang
Santa Clara University, cyang@scu.edu

D. S. Sugiharto

A. S. Byrne

M. Ju

See next page for additional authors

Follow this and additional works at: https://scholarcommons.scu.edu/elec

Part of the Electrical and Computer Engineering Commons

Recommended Citation
M.M. Rahman, C.Y. Yang, D. Sugiarto, A.S. Byrne, M. Ju, K. Tran, K.H. Lui, T. Asano, and W.F. Stickle, "Properties and Device Applications of Hydrogenated Amorphous Silicon Carbide Films," Journal of Applied Physics 67, 7065- 7070 (1990). https://doi.org/10.1063/1.345055

Copyright © 1990 American Institute of Physics Publishing. Reprinted with permission.

This Article is brought to you for free and open access by the School of Engineering at Scholar Commons. It has been accepted for inclusion in Electrical Engineering by an authorized administrator of Scholar Commons. For more information, please contact rscroggin@scu.edu.

Authors
M. Mahmudur Rahman, Cary Y. Yang, D. S. Sugiharto, A. S. Byrne, M. Ju, K. Tran, and K. H. Lui

This article is available at Scholar Commons: https://scholarcommons.scu.edu/elec/79

Properties and device applications of hydrogenated amorphous silicon carbide films

M. M. Rahman, C. Y. Yang, D. Sugiarto, A. S. Byrne,[a] M. Ju, K. Tran, and K. H. Lui
Microelectronics Laboratory, Santa Clara University, Santa Clara, California 95053

T. Asano
Department of Computer Science and Electronics, Kyushu Institute of Technology, Iizuka, Fukuoka 820, Japan

W. F. Stickle
Perkin-Elmer, Physical Electronics Laboratory, Eden Prairie, Minnesota 55344

(Received 11 September 1989; accepted for publication 9 February 1990)

Hydrogenated amorphous silicon carbide (*a*-SiC:H) films were deposited with a radio-frequency plasma-enhanced chemical vapor deposition system which utilizes a dc electric field applied independently of the inductively coupled rf field. The source gases were SiH_4 and CH_4. It was found that application of an electric field directed out of the substrate surface enhances the growth rate and yields some improvements in photoconductivity. The compositions of the films were evaluated by x-ray photoelectron spectroscopy for a range of source gas mixtures. In order to assess the applicability of *a*-SiC:H thin films, heterojunction *a*-SiC:H/crystalline Si (*c*-Si) diodes were fabricated and their electrical characteristics evaluated. The diode capacitance-voltage results confirmed a step junction, which was consistent with the abruptness of the interface demonstrated by high-resolution transmission electron microscopy. The heterojunction diodes also showed good rectifying properties, suggesting promise for *a*-SiC:H in device applications.

I. INTRODUCTION

The study of hydrogenated amorphous silicon carbide (*a*-SiC:H) is motivated by its potential in applications such as emitter material in heterojunction bipolar transistors (HBT), thin-film solar cells, image sensors, photoreceptors, near-visible electroluminescence devices, phototransistors, color sensors, and light-emitting diodes in the visible range.[1-10] Its optical band gap can be continuously controlled by changing the alloy composition.[11-13] Low-resistivity *a*-SiC:H film is a good candidate as the emitter in high-frequency, high-speed Si HBT because of low processing temperature and expected lower interface state density at the heterojunction than crystalline materials.[14-16]

Amorphous SiC:H layers deposited in CH_4/SiH_4 mixtures incorporate carbon mostly in the form of CH_3 groups.[17-21] Since these groups do not contribute to the bridging network, the deterioration of electronic properties with increasing concentration of CH_3 groups is caused by an increase in local voids and the formation of polysilane chains and dangling bonds.[22] In view of this inhomogeneous nature of *a*-SiC:H, the mobilities of carriers are considerably less than those in crystalline SiC.

It has been shown that the mobility band gap of *a*-SiC:H is to a large extent determined by the carbon incorporated in the Si—CH_3 configuration.[23] CH_x and SiH_y bonding configurations may cause an inhomogeneous modulated band-edge structure, resulting in low carrier mobility and low doping efficiency. Therefore, to enhance film quality, it is essential to incorporate carbon atoms in the form of a Si-C network, minimizing the band-edge modulation.

Since in the plasma a C—H bond ($\sim$4.5 eV) is less likely broken than a Si—H ($\sim$4 eV) or Si—C bond ($\sim$3.7 eV), one approach to reduce the fraction of CH_3 groups in the film is to use disilylmethane (DSM).[24] However, DSM-produced films only show higher photoconductivity for optical band gaps larger than 2 eV.

It has also been shown that electron bombardment is effective in growing diamond films from CH_4.[25] This suggests that C—H bonds can be effectively dissociated by electron bombardment during the growth process.

One objective of the present work was to study the growth mechanism and electrical and optical properties of device-quality *a*-SiC:H films fabricated with a SiH_4/CH_4 mixture, when a dc field is applied as in the case of diamond films. This dc field is expected to increase dissociation of source gases through enhanced electron bombardment of the surface, resulting in higher concentration of Si—C bonds in the films. In order to apply this technique to the formation of *a*-SiC:H films, we have constructed an rf PECVD system in which a longitudinal dc electric field is applied across the plasma, independent of the rf field. This configuration is similar to the so-called cross-field PECVD system[26] with the rf field coupled inductively. In this report we show that the growth characteristics and properties of *a*-SiC:H films are indeed controlled to a large extent by the dc field.

In addition to acceptable film properties, the application of *a*-SiC:H to heterojunction devices requires suitable interface properties as well. A recent study revealed that the current gain in a Si HBT with an *a*-SiC:H emitter and low base dopant concentration was improved by hydrogen ter-

---

[a] Current address: Hitachi Research Laboratory, Hitachi, Ltd., 4026 Kuji-cho, Hitachi, Ibaraki 319-12, Japan.

 0021-8979/90/117065-06$03.00 © 1990 American Institute of Physics

minators at the interface.[14] In preparing our samples we have used source gases diluted to 1%–5% in H_2 to achieve similar effects. Other researchers have found that in amorphous silicon (*a*-Si:H)/*c*-Si heterostructures produced by PECVD method, the deposited *a*-Si:H epitaxially crystallizes near the interface, although the film was deposited under conditions favorable for abrupt amorphous/crystalline junction formation.[27,28] The observed thickness of the epitaxially crystallized region in the deposited *a*-Si:H films was at least 10 nm. Such epitaxial crystallization modifies the energy-band structure of the heterostructure and leads to complex electrical behavior.[14] This phenomenon exhibited by *a*-Si:H films leads us to probe for similar behavior in *a*-SiC:H/*c*-Si. The high-resolution transmission electron microscopy (HRTEM) study of such interfaces revealed abrupt junctions in contrast to the *a*-Si:H result.

Finally, in order to assess the utility of *a*-SiC:H in device applications, *a*-SiC:H/*c*-Si heterojunction diodes were fabricated and their electrical characteristics evaluated. The capacitance-voltage characteristics revealed a step junction, which was consistent with HRTEM results for the interface. The diodes also showed good rectifying properties suggesting promise as emitter-base junctions in HBTs.

II. EXPERIMENT

Figure 1 shows a diagram of the field-enhanced PECVD system used where the rf power at 13.56 MHz is inductively coupled to the reactor. The quartz reactor contains two parallel metal plates serving as dc electrodes with one being the substrate holder. Source gases were SiH_4 and CH_4, each diluted to 5% in H_2, supplied through mass-flow controllers which maintained a gas flow-rate ratio $R = CH_4/(SiH_4 + CH_4)$ varied from 0% to 75% and a reactor pressure of about 0.5 Torr. Films were grown with substrate temperatures ranging from 200 °C–500 °C with the rf power fixed at 50 W. From the diameter of the cylindrical deposition chamber, $d = 150$ mm, the average power density in the deposition chamber is estimated to be 0.28 W/cm^2 at 50 W. The applied dc voltage ranged from -300 V (electric field $= -60$ V/cm) to $+250$ V (electric field $= +50$ V/cm) with current densities of -2 mA/cm^2 and $+1.5$ mA/cm^2, respectively. Quartz and *p*-Si (111) substrates used for this experiment were cleaned in $NH_4OH:H_2O_2:H_2O$ and $HCl:H_2O_2:H_2O$ solutions. The substrates for XPS composition measurements were oxidized *p*-Si (111) wafers and quartz.

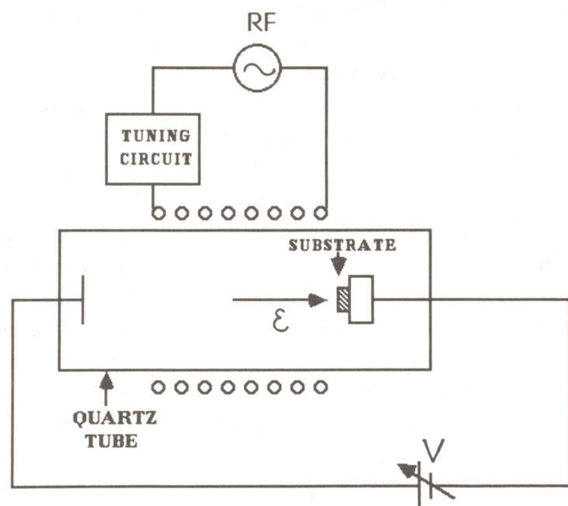

FIG. 1. Schematic of the field-enhanced PECVD system.

Thicknesses of films grown on quartz substrates were measured by a spectrophotometer. Thicknesses of films grown on crystalline Si substrates were measured using an ellipsometer and a spectrophotometer.

Atomic concentrations were computed from high-resolution XPS spectra taken after ion-etching 7 nm of material and are based on peak areas and elemental sensitivity factors. The XPS data were acquired with a spectrometer using a monochromated Al x-ray source. All XPS data were taken with a sample angle of 45° with respect to the analyzer.

For room-temperature dark conductivity measurements, 500-nm-thick aluminum electrode patterns were deposited on top of the films. The current-voltage characteristics of the electrode pairs were measured with a semiconductor parameter analyzer. For photoconductivity measurements, an ultraviolet light source was used. The optical band gap was estimated using the $\sqrt{\alpha h\nu}$ vs $h\nu$ ($\alpha =$ absorption coefficient, $h\nu =$ photon energy) relation derived from transmission spectra obtained with a spectrophotometer and following the analysis of Tauc[29] and Davis and Mott.[30]

For HRTEM studies of the *a*-SiC:H/*c*-Si interface, silicon (111) wafers were cleaned with organic solvents and $NH_4OH:H_2O_2:H_2O$ and $HCl:H_2O_2:H_2O$ solutions. The native oxide was removed in an HF dip immediately before sample loading. The *a*-SiC:H films were then deposited on the Si wafers at 300 °C with no dc bias. Cross-sectional HRTEM samples were prepared through slicing, mechanical polishing, and Ar-ion milling processes. HRTEM observations were carried out with a JEOL-200CX which had point-to-point resolution of about 0.21 nm.

Heterojunction *a*-SiC:H/*c*-Si mesa diodes having cross-sectional areas of 0.02 cm^2 were fabricated by depositing phosphorus-doped *a*-SiC:H films at zero dc voltage on a 17 Ω cm *p*-Si (111) substrate. 1% PH_3 diluted in H_2 was added to SiH_4 and CH_4 gases to form the n^+ *a*-SiC:H layer. Aluminum back contacts were then deposited. The native oxide was removed with an HF dip, followed by Al deposition through a dot-patterned hard mask to form the top electrode. The specimen was then subjected to CF_4 plasma etching to form a mesa structure. Current-voltage and capacitance-voltage characteristics were measured using a semiconductor parameter analyzer and an impedance analyzer, respectively.

III. RESULTS AND DISCUSSION

A. Growth characteristics

Figure 2 shows Arrhenius plots of average growth rates for *a*-SiC:H films deposited under various dc fields. The behaviors for the two substrate temperature ranges, 200 °C-300 °C and 300 °C–500 °C, are discussed separately.

In the temperature range 200 °C–300 °C, for zero field

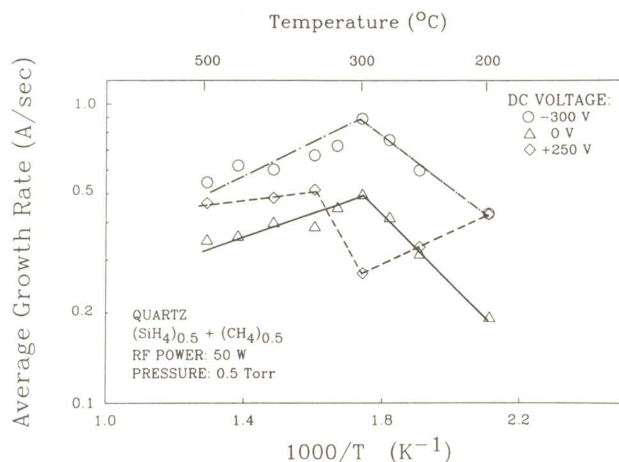

FIG. 2. Arrhenius plot of average growth rate of *a*-SiC:H films for several dc fields.

the growth rate increases with increasing substrate temperature. The activation energy obtained from this plot is 0.22 eV. For a field of 60 V/cm directed out of the substrate (negative field), the growth rate is enhanced and the activation energy is reduced to 0.17 eV. The results for negative field follow a pattern similar to that for zero field. On the other hand, for a positive field of 50 V/cm, the growth rate decreases with increasing substrate temperature.

The results in the 200 °C–300 °C temperature range indicate that while dissociation of molecules and/or radicals adsorbed to the substrate surface and subsequent growth are assisted by electron bombardment due to the negative field, dissociation *and* evaporation of these adsorbates are enhanced by proton bombardment when the field direction is reversed.[31] The former phenomenon is illustrated in Fig. 3. The reduction in activation energy for negative field suggests that the electron bombardment associated with this field is able to assist to a greater extent the thermally activated processes involved in the film growth. The growth enhancement by either electron or proton bombardment is more significant at 200 °C substrate temperature since the thermal energy is not sufficiently high to dissociate or desorb the adsorbed species. It has been shown that hydrogen ion bombardment increases the rate of evaporation of adsorbed species[28] by etching out weakly bonded radicals at the surface, resulting in a denser random network.[32] Thus the observed decrease in growth rate with increasing substrate temperature for positive field is attributed to an increasing number of protons striking the surface.

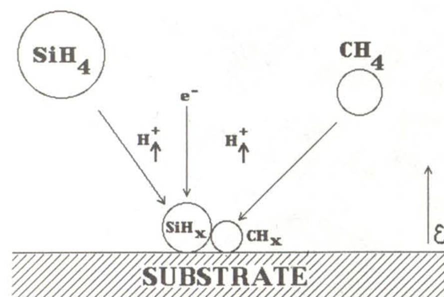

FIG. 3. Schematic of the deposition system illustrating the effects of the applied dc field.

In the 300 °C–500 °C temperature range, growth rates show a slightly decreasing trend for all dc field conditions. We attribute this to the formation of structures other than amorphous, and/or temperature-dependent etching reactions at the surface. The growth rate is enhanced by both positive and negative fields. In fact, these rates start to converge at 500 °C. This result demonstrates that at high substrate temperatures the choice of polarity of the dc field is inconsequential and that the film growth is dominated by thermally activated processes brought about by high substrate temperatures. The growth rate for positive field is lower than that for negative field, consistent with enhanced evaporation due to proton bombardment for positive fields.

Our experiments have demonstrated that the film growth rate depends critically on substrate temperature, dc field, substrate structure, and rf power. The detailed chemical reactions in this multicontrolling-parameter process are complex and our results suggest a combination of simultaneous deposition and etching reactions throughout the entire temperature range. At low substrate temperatures, 200 °C–300 °C, etching is dominated by deposition and the growth behavior for zero and negative fields is Arrhenius-like. Negative field enhances deposition while positive field assists in etching and evaporation, resulting in a negative activation energy. At higher substrate temperatures, etching becomes comparable to deposition, and the dc field effect is less significant, so that their combination results in decreasing growth rate with increasing temperature regardless of dc field.

B. Chemical composition

XPS measurements were performed to obtain carbon and silicon contents for films grown at zero dc field on oxidized Si wafers. These data were taken for films grown at an rf power of 50 W and a substrate temperature of 300 °C. In Table I, the carbon/silicon ratio for the *a*-SiC:H films show, as expected, that carbon content increases with increasing CH_4/SiH_4 ratio.[33] An increase in methane content is also expected to result in corresponding increase in concentration of carbon polyhydride (CH_2, CH_3) configurations, which degrade the quality of the films.[17–21] Traces of oxygen ($\lesssim 8\%$) were also detected in the films and are due to unwanted oxygen present in the chamber during deposition. Whereas the films grown on oxidized *c*-Si substrates showed a Si content of 77% at a CH_4/SiH_4 ratio of unity and an rf power of 50 W, those grown on quartz under the same conditions yielded 82%. This finding further confirms that the film properties are dependent on the exact nature of the surface reactions during the growth process.

TABLE I. Methane/silane ratio in the gas mixture and carbon/silicon ratio in the *a*-SiC:H films grown on oxidized crystalline Si substrates. rf power = 50 W. Substrate temperature = 300 °C.

CH_4/SiH_4	0	0.49	1	1.5	1.86	3
C/Si	0	0.095	0.195	0.257	0.324	0.517

C. Optical and electrical properties

Figure 4 shows the optical band gap of the films as a function of substrate temperature and applied dc field. The results indicate that negative field reduces optical band gap for substrate temperatures up to 300 °C. In these films, the dissociation enhancement due to electron bombardment brought about by the negative field is expected to reduce CH_x and SiH_y bonding configurations in the film. Thus, more Si—C bonds are formed, resulting in less band-edge modulation and smaller optical bandgap. On the other hand, positive field reduction in band gap was observed for films deposited at 200 °C, and enlargement at 250 °C and 300 °C. Thus no clear trend for band-gap variation is evident for positive fields in this temperature range.

It has been shown recently that an increase in the optical band gap is primarily governed by increasing hydrogen content[34] and that a higher density of Si—C and Si—Si bonding networks results in less hydrogen incorporation and vice versa.[32,35] As shown in Fig. 4, the films grown at 500 °C have optical band gaps markedly lower than those deposited at lower temperatures. This suggests less hydrogen incorporation, resulting in more Si—C and Si—Si bonds. For this substrate temperature, the optical band gap increases with negative field and varies little with positive field. This is consistent with the notion that while electron bombardment enhances growth at low temperatures by dissociating adsorbed species, at higher temperatures it also plays a role in dissociating bonds formed at and near the surface, such as Si—C and Si—Si.

Figure 5 shows the measured photoconductivity as a function of substrate temperature and dc field. The dark conductivity in each case is approximately 10^{-9} S/cm. At low substrate temperature (200 °C), the photoconductivities are the lowest for all fields. This suggests that band-edge modulation is large, which correlates well with the wide optical band gaps ($\sim$2 eV) shown in Fig. 4. At 300 °C substrate temperature, higher photoconductivity is obtained; and at a dc field of $-$ 60 V/cm, the value increases fivefold from the zero field one. This increase suggests that the film formed under negative field has less band-edge modulation, consistent with the optical band-gap results. At 500 °C, the photoconductivity decreases with negative field, again consistent with optical band-gap behavior. The decrease in photoconductivity with positive field for each temperature is attributed to an increase in hydrogen concentration in the film[32] over the zero field case. This increased hydrogen concentration tends to reduce the number of unsaturated bonds and thus the availability of free carriers.

Our data on growth rate, optical band gap, and photoconductivity seem to point collectively toward an optimum deposition temperature of 300 °C with an electric field of at least 60 V/cm directed out of the substrate surface.

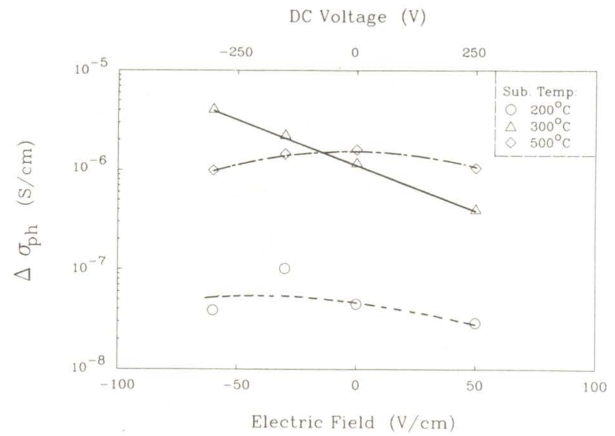

FIG. 5. $\Delta\sigma_{ph}$ (photoconductivity-dark conductivity) of *a*-SiC:H films as a function of dc field and substrate temperature.

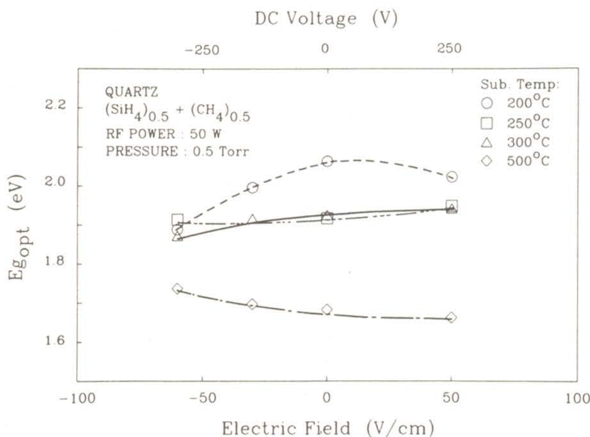

FIG. 4. Optical band gap of *a*-SiC:H films as a function of dc field and substrate temperature.

D. Interface structure

Figure 6 shows a cross-sectional HRTEM image of an *a*-SiC:H/*c*-Si (111) specimen. This micrograph reveals an abrupt interface, with a maximum asperity of three atomic planes. This asperity is attributed to substrate etching in the early stages of film growth. The interface morphology demonstrates that, in contrast to the *a*-Si:H/*c*-Si heterostructures,[27,28] epitaxial growth does not take place in *a*-SiC:H films grown on *c*-Si substrates by using a conventional PECVD method. When the dc field is applied, the resulting drift motion of the ionized species may enhance the etching process as illustrated in Fig. 3, resulting in more pronounced interfacial asperity. HRTEM results for films deposited with $-$ 60 V/cm of applied field showed that the interfacial as-

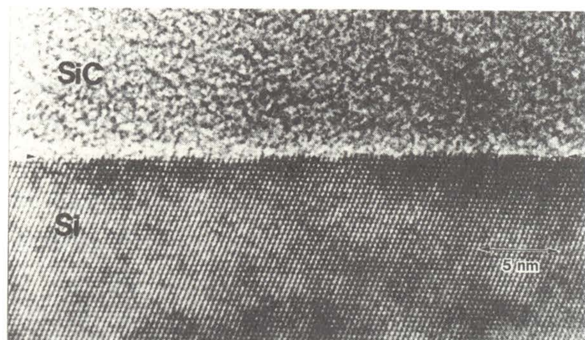

FIG. 6. HRTEM cross-sectional image of an *a*-SiC:H/*c*-Si (111) interface taken along a ⟨011⟩ direction.

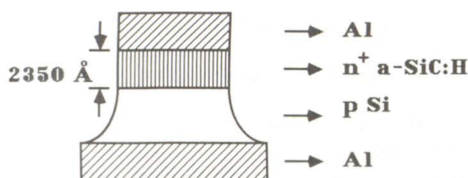

FIG. 7. Schematic of the *a*-SiC:H/*c*-Si heterostructure diode.

perity almost doubled that for films grown with no dc field.[36]

Epitaxial crystallization is generally associated with interfacial contamination such as oxide. If there is an oxide layer, a bright band would appear at the interface in the micrograph since the density of amorphous SiO_2 is less than that of *a*-SiC:H. No such feature is visible at the interface shown in Fig. 6, although we did not profile the oxygen concentration. We have observed the existence of oxide layers in other samples and found that their presence is sensitive to sample treatment before loading into the deposition system. For preparation of the specimen shown in Fig. 6, care was taken to minimize the time between the HF dip and pumping down the reaction chamber.

E. Diode characteristics

Figure 7 shows the schematic of the diode structure. Capacitance-voltage results of the *a*-SiC:H/*c*-Si n^+p heterojunction diodes obtained at 1 MHz are shown in Fig. 8. The dark conductivity of a phosphorus-doped film grown on quartz substrate under identical conditions was measured to be 9×10^{-4} S/cm. The $1/C^2$ versus bias plot shows two linear regions, A and B. Region A confirms a step junction, which is consistent with the HRTEM results for the interface. A built-in voltage of 0.8 V is extrapolated from region A. The substrate dopant concentration profile from the interface calculated from the *C-V* characteristics[37] is shown in the inset of Fig. 8. The calculated substrate impurity concentration of $10^{15}/cm^3$ is consistent with the wafer resistivity of 17 Ω cm obtained with four-point probe measurement. Region B is due to concentration variation in the substrate as confirmed by spreading resistance measurements and is not a consequence of the deposition process.

Figure 9 shows the current-voltage characteristics of a representative diode with an ideality factor of 1.58 for forward biases of up to 0.4 V. This suggests that the density of carrier recombination centers at the interface is fairly low. The diode has good rectifying properties and a reverse-biased current density of 1.58×10^{-7} A/cm^2 was obtained at 0.5 V. These results indicate that the *a*-SiC:H/*c*-Si heterojunction possesses electrical properties suitable for HBT applications. The diodes were fabricated from *a*-SiC:H with films produced under zero dc field. Fabrication and characterization of diodes from films produced under negative fields are in progress.

IV. SUMMARY AND CONCLUSION

A novel rf PECVD system has been developed in which a dc electric field is applied independently of the inductively coupled RF field. It has been found that for *a*-SiC:H the average growth rate, optical band gap, and photoconductivity were altered substantially by the dc field, and they generally improved for films formed by applying an electric field directed out of the substrate surface. These improvements are attributed to enhanced dissociation of adsorbed source gas molecules due to increased electron bombardment. The optical band-gap data correlate quite well with measured photoconductivity for negative fields.

It has been found from HRTEM observations that, in contrast with *a*-Si:H/*c*-Si, a fairly abrupt amorphous/crystal interface is formed in the *a*-SiC:H/*c*-Si heterostructure. This result indicates that the band structure of *a*-SiC:H near the interface is similar to that in the bulk, and that we can tailor the composition of the films to the desired band structure of the *a*-SiC:H/*c*-Si heterojunction.

The n^+p *a*-SiC:H/*c*-Si (111) heterostructure diodes showed good rectifying properties with ideality factors suggesting low concentration of interface recombination centers. The *C-V* characteristics of the diodes confirm that the junction is electrically abrupt. These results are encouraging for realizing an n^+pn *a*-SiC:H/*c*-Si HBT.

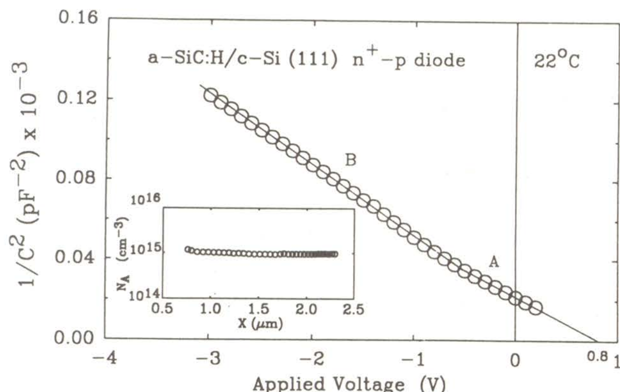

FIG. 8. Capacitance-voltage characteristics of an n^+p *a*-SiC:H/*c*-Si diode. Doping profile in *c*-Si calculated from the *C-V* data is shown in the inset, where $X = 0$ corresponds to the interface.

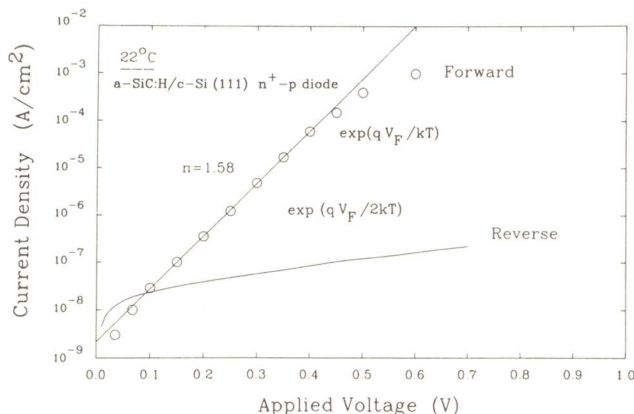

FIG. 9. Current-voltage characteristics of an n^+p *a*-SiC:H/*c*-Si (111) diode.

ACKNOWLEDGMENTS

The authors gratefully acknowledge Dr. F. A. Ponce of Xerox-PARC for valuable discussions and preparation of the HRTEM samples and the HRTEM images of the *a*-SiC:H/*c*-Si heterostructures. This work was supported in part by the Perkin-Elmer Corporation. The authors also wish to thank Dr. C. C. Tsai of Xerox-PARC for assistance in plasma etching of the diodes and for useful suggestions. The authors are thankful to Richard Williams of Siliconix for providing the SRP results.

[1] K. Sasaki, S. Furukawa, and M. M. Rahman, Tech. Dig. IEDM '85, 294 (1985).
[2] Y. Tawada, H. Okamoto, and Y. Hamakawa, Appl. Phys. Lett. **39**, 237 (1981).
[3] M. M. Rahman and S. Furukawa, Electron. Lett. **20**, 57 (1984).
[4] H. Kurihara, T. Takeshita, and Y. Machida, in *Amorphous Silicon Technology-1989*, edited by A. Madan, M. J. Thompson, P. C. Taylor, Y. Hamakawa, and P. G. LeComber (Materials Research Society, Pittsburgh, PA, 1989), MRS Symp. Proc. Vol. 149, p. 221.
[5] Y. Nakayama and S. Akita, in *Amorphous Silicon Technology-1989*, edited by A. Madan, M. J. Thompson, P. C. Taylor, Y. Hamakawa, and P. G. LeComber (Materials Research Society, Pittsburgh, PA, 1989), MRS Symp. Proc. Vol. 149, p. 645.
[6] H. Munekata and H. Kukimoto, Appl. Phys. Lett. **42**, 432 (1983).
[7] C. Y. Chang, B. S. Wu, Y. K. Fang, and R. H. Lee, Appl. Phys. Lett. **47**, 49 (1985).
[8] K. C. Chang, C. Y. Chang, Y. K. Fang, and S. C. Jwo, IEEE Electron Device Lett. **EDL-8**, 64 (1987).
[9] H. K. Tsai, S. C. Lee, and W. L. Lin, IEEE Electron Device Lett. **EDL-8**, 365 (1987).
[10] D. Kruangam, T. Endo, G. P. Wei, S. Nonomura, H. Okamoto, and Y. Hamakawa, J. Non-Cryst. Solids **77 & 78**, 1429 (1985).
[11] D. A. Anderson and W. E. Spear, Philos. Mag. **35**, 1 (1976).
[12] T. Shimada, Y. Katayama, and K. F. Komatsubara, J. Appl. Phys. **50**, 5530 (1979).
[13] B. von Roedern, D. K. Paul, J. Blake, R. W. Collins, G. Moddel, and W. Paul, Phys. Rev. B **25**, 7678 (1982).
[14] M. Kuwagaki, K. Imai, T. Ogino, and Y. Amemiya, Jpn. J. Appl. Phys. **28**, L173 (1989).
[15] T. Sugii, T. Ito, Y. Furumura, F. Mieno, and M. Maeda, IEEE Electron Device Lett. **9**, 87 (1988).
[16] K. Sasaki, T. Fukazawa, and S. Furukawa, Tech. Dig. IEDM, Washington, DC, 186 (1987).
[17] W. Beyer, H. Wagner, and H. Mell, Mater. Res. Soc. Symp. **49**, 189 (1985).
[18] Y. Tawada, K. Tsuge, M. Kondo, H. Okamoto, and Y. Hamakawa, J. Appl. Phys. **53**, 5273 (1982).
[19] A. H. Mahan, P. Raboisson, and R. Tsu, Appl. Phys. Lett. **50**, 335 (1987).
[20] I. Solomon, M. P. Schmidt, and H. Tranc-Ouoc, Phys. Rev. B **38**, 9895 (1988).
[21] J. Sotiropoulos and G. Weiser, J. Non-Cryst. Solids **92**, 95 (1987).
[22] H. -K. Tsai, W. -L. Lin, W. J. Sah, and S. -C. Lee, J. Appl. Phys. **64**, 1910 (1988).
[23] W. J. Sah, H. K. Tsai, and S. C. Lee, in *Extended Abstracts of the 20th (1988 International) Conference on Solid State Devices and Materials* (Japan Society of Applied Physics, Tokyo, 1988), p. 243.
[24] W. Beyer, R. Hager, H. Schmidbaur, and G. Winterling, Appl. Phys. Lett. **54**, 1666 (1989).
[25] A. Sawabe and T. Inuzuka, Appl. Phys. Lett. **46**, 146 (1985).
[26] H. Okamoto, T. Yamaguchi, and Y. Hamakawa, J. Non-Cryst. Solids **35 & 36**, 201 (1980).
[27] K. Baert, J. Symons, W. Vandervorst, J. Vanhellemont, M. Caymax, J. Poortmans, J. Nijs, and R. Mertens, Appl. Phys. Lett. **51**, 1922 (1987).
[28] T. Uematsu, S. Matsubara, M. Kondo, M. Tamura, and T. Saitoh, Jpn. J. Appl. Phys. **27**, L493 (1988).
[29] J. Tauc, in *Amorphous and Liquid Semiconductors*, edited by J. Tauc (Plenum, New York, 1974), Chap. 4.
[30] E. A. Davis and N. F. Mott, Philos. Mag. **22**, 903 (1970).
[31] C. C. Tsai, in *Amorphous Silicon and Related Materials*, edited by H. Fritzsche (World Scientific, Singapore, 1989), Vol. 1, p. 123.
[32] A. Matsuda, T. Yamaoka, S. Wolff, M. Koyama, Y. Imanishi, H. Kataoka, H. Matsuura, and K. Tanaka, J. Appl. Phys. **60**, 4025 (1986); A. Matsuda and K. Tanaka, J. Non-Cryst. Solids **97-98**, 1367 (1987).
[33] M. M. Rahman and S. Furukawa, Jpn. J. Appl. Phys. **23**, 515 (1984).
[34] W. Beyer, H. Wagner, and H. Mell, in *Materials Issues in Applications of Amorphous Silicon Technology*, edited by D. Adler, A. Madan, and M. J. Thompson (Materials Research Society, Pittsburgh, PA, 1985), MRS Symp. Proc. Vol. 49, p. 189.
[35] A. Matsuda, M. Koyama, N. Ikuchi, Y. Imanishi, and K. Tanaka, Jpn. J. Appl. Phys. **25**, L54 (1986).
[36] A. S. Byrne, Y. Misawa, M. Nakamura, T. Suzuki, T. Asano, H. Lui, D. Sugiarto, K. Tran, M. Rahman, and C. Yang, "Growth Characteristics of Amorphous Silicon Carbide on Crystalline Silicon Substrates," to be presented at the Spring meeting of the ECS, Montreal, Quebec, May 6–11, 1990.
[37] R. S. Muller and T. I. Kamins, in *Device Electronics for Integrated Circuit* 2nd ed. (Wiley, New York, 1986), p. 193.